2-8-2023

Study of the graphene energy absorbing layer and the viscosity of sodium alginate in Laser-Induced- Forward-Transfer (LIFT) bioprinting

Shuqi Zhou

Jianzhi Li

Ben Xu

Proceedings of the ASME 2022
International Mechanical Engineering Congress and Exposition
IMECE2022
October 30-November 3, 2022, Columbus, Ohio

IMECE2022-96190

Study of the graphene energy absorbing layer and the viscosity of sodium alginate in Laser-Induced-Forward-Transfer (LIFT) bioprinting

Shuqi Zhou
Department of Mechanical Engineering, Mississippi State University, Mississippi State, MS, 39762

Jianzhi Li
Department of Manufacturing and Industrial Engineering, University of Texas Rio Grande Valley, Edinburg, TX 78539

Ben Xu*
Department of Mechanical Engineering, Mississippi State University, Mississippi State, MS, 39762
xu@me.msstate.edu

ABSTRACT

Laser induced forward transfer (LIFT) bioprinting has been viewed as a new and actively developed three-dimensional bioprinting technology due to its high accuracy and good cell viability. The printing quality is highly dependent on the jet formation and its stability in the LIFT bioprinting process. The objective of this study is to investigate the effect of a graphene Energy Absorbing Layer (EAL) and alginate hydrogel (SA) (w.t. 1% and 2%) viscosity on jet generation in the LIFT bioprinting process. Since SA exhibits a shear-thinning behavior, it is a non-Newtonian fluid. The effect of EAL thickness and SA's viscosity were addressed for various experimental conditions. After the laser irradiated on the quartz substrate, small holes caused by laser interaction appeared in the interaction area on the EAL. The EAL substrate with multiple holes was examined using an optical microscope, and the morphology of holes was observed and compared. The images of jet generation showed that graphene EAL can assist in the transfer of SA with a low laser energy absorption rate. The viscosity of the SA also plays a significant role in the generation of a stable jet for SA transfer. For the cases with the same laser energy input, the jet generated using higher viscosity bioink had a smaller initial velocity, which eventually led to a shorter jet length. The findings in this study will facilitate the development of new EAL in LIFT bioprinting.

Keywords

Bioprinting, Laser Induced Forward Transfer (LIFT), Energy Absorbing Layer (EAL), Sodium Alginate (SA)

1. INTRODUCTION

Three-dimensional (3D) bioprinting is an emerging technology that covers the knowledge of biology, materials science, and engineering [1, 2]. It has been widely adopted in the field of regenerative medicines and tissue engineering [3]. Bioprinting can be classified into three major categories, inkjet bioprinting, extrusion bioprinting, and laser-assisted bioprinting (LAB) [4]. Laser-Induced-Forward-Transfer (LIFT) bioprinting is one of the LAB technologies which has several unique advantages, such as high printing accuracy, no nozzle clogging, and high cell viability [5-7]. However, LIFT bioprinting still has several issues that cannot be easily ignored, for example its printing quality highly depends on the stable jet regime, which is related to the rheological and mechanical properties of the bioink and the laser process parameters [7, 8]. It has been reported that the interaction between the laser and bioink is crucial for the bioprinting process since it strongly affects the bubble generation and jet formation process [9]. Some numerical models have been developed to predict the multiphase process in LIFT and optimize the printing parameters in order to obtain a good printing quality [10].

There are several different ways to improve the printing quality in LIFT, adopting an energy absorbing layer (EAL) between the transparent quartz and the bioink layer is one of them, as shown in **Figure 1**. The benefit of having an EAL is to actuate the flow of bioink and stabilize the jet regime. Based on literature review, some researchers studied the effect of various EAL materials, such as Ag, Au, Ti, and TiO [11-16]. Another potential benefit is that the addition of EAL can improve the laser-absorbing rate, and prevent the direct contact of bioink from the laser beam, thus can improve the cell viability [13]. However, research have shown that with Ag and Au as the EAL,

the EAL will break and the ruptured debris may be ejected into the droplet during the LIFT process, the further negative impact of the metallic debris on the cell growing process of LIFT has not been fully understood yet [17-19], but it can be found from both *in-vivo* and *in-vitro* biomedical research that the micro and nano scale metallic particles will trigger abnormal immune responses [20], which is definitely not desired in the post-printing stages. There is limited research on inorganic non-metallic materials as EAL, when compared to metallic EAL, for example graphene exhibits good biocompatibility, it has been widely used in the field of biosensors and biomedical engineering [21, 22], and therefore graphene can be a potential material as the EAL in LIFT. A good design of EAL can critically affect the printing resolution and ultimately advance the cell viability. Therefore, evaluating the effect of EAL on the jet regime in the LIFT process is vital to the development of next generation of high efficiency and high throughput LIFT bioprinting.

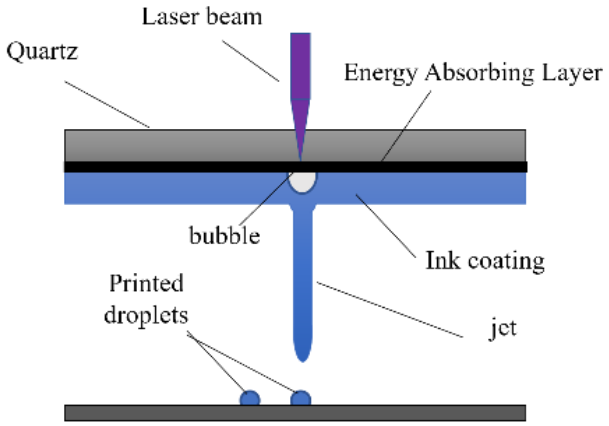

***Fig. 1**. Schematic of LIFT printing process with EAL*

Bioink is any natural or synthetic polymer selected for its biocompatible components and favorable properties. Bioink can be composed only of live cells, but in most cases, an additional carrier material that envelops the cells is also added. This carrier material is usually a biopolymer gel, such as hydrogel, which acts as a 3D molecular scaffold. Therefore, the rheological property of bioink plays a significant role in the LIFT printing process [23, 24]. Most biological fluids are non-Newtonian [25], which behave quite differently from Newtonian fluids in the multiphase process. Therefore, testing the viscosity of bioink is an important step to evaluate the quality of LIFT printing.

It is important the note that no cells were involved in this study, only hydrogel was utilized to be coated on the quartz for material transfer, because adding live cells or not will not significantly affect the rheology of hydrogel and the laser-induced multiphase process. Therefore, this study can discover major findings about the benefits of adopting a graphene based EAL, particularly the laser-induced jet development and the effects on the EAL itself after the printing. The objectives of this study are: (1) to demonstrate the effect of applying graphene EAL and the influence of EAL thickness on the jet regime in the LIFT process; (2) to illustrate the differences of generated jets between two SA solutions. The shape of the jet regime is also used to evaluate the printing performance, and the microscope images of the EAL after the laser interactions are also discussed.

It is hoped that the findings in this study will facilitate the development of new EAL for LIFT bioprinting, and the results will also help the bioprinting research community to achieve higher cell viability in bioprinting.

2. MATERIALS AND METHODS

2.1 Laser printing apparatus

The in-house customized LIFT printing platform is shown in **Figure 2 (a)**. In this platform, the pulse laser is generated by a laser generator (Spirit One 1040–8), and Gaussian distribution can be used to describe the laser intensity here. The laser's wavelength is 1040nm, the maximum pulse laser energy we used here is 30 μJ, and the pulse duration is 300 fs. During the printing process, the laser pulse generated from the laser generator is reflected by several optics, then passes the galvanometer, until it concentrates on the transparent ribbon/quartz, and then interacts with the liquid. During the printing process, an XY stage (Pro115LM Aerotech) is utilized to move the ribbon and the substrate structure. A sharp background was provided by a light source (HL150-A Fisher Scientific). The whole printing process is recorded by a high-speed camera (Phantom VEO 410L). In this study, the frame rate was set as 110000 fps, which means the interval of each frame is about 9.09 μs, and the exposure time was fixed as 8 μs. An optical microscope (Axiovert 200 M) was later utilized to measure the thickness of EAL and observe the morphology of the holes in the energy absorbing layer after the printing process.

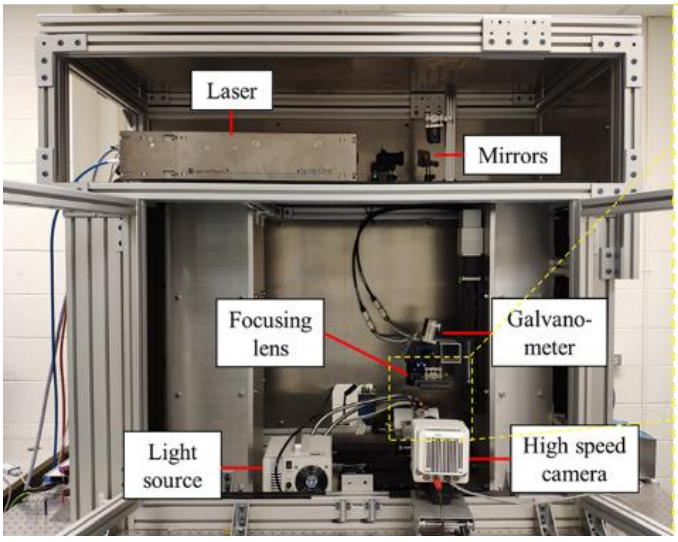

(a)

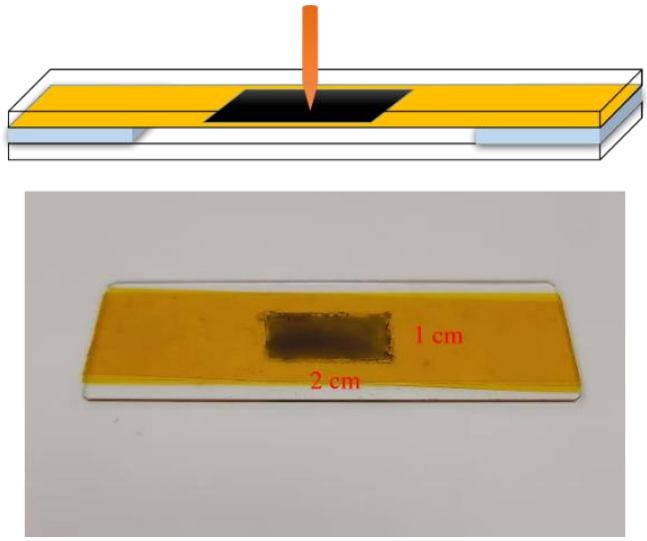

(b)

Fig. 2. *(a) Experimental platform for LIFT process. (b) Donor preparation*

2.2 Graphene EAL and bioink preparation

The structure of the ribbon is shown in **Figure 2 (b)**. In this study, the bottom side of the quartz was covered by a yellow tape, and the central area of the table was then removed. The thickness of the quartz was set as 50 μm and the thickness of each layer of tape attached to the quartz was 50 μm, therefore the size of the removed area was 20 mm by 10 mm. 1 wt% graphene disperse solution was added to the central area without covering tape, and then another slide glass was used to scrape over the central area filled with graphene solution, in order to maintain a smooth finish. The prepared EAL samples were then placed in a sealed chamber with controlled temperature and relative humidity for 2 hours to obtain completely dried EAL samples.

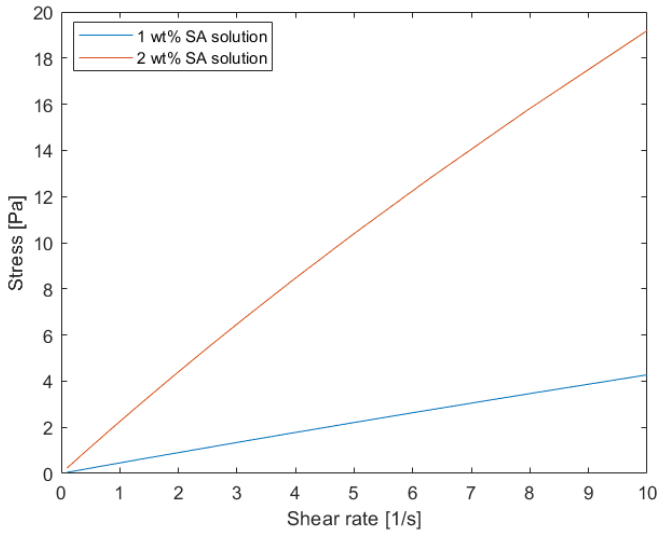

Fig. 3. *Flow behaviors of 1% SA solution and 2% SA solution*

SA powders (American Heritage Industries, Cleveland, OH) were dissolved in deionized water with concentrations of 1wt% and 2wt% to make the cell-free bioinks. The viscosity of both SA solutions was tested using Discovery HR-2 hybrid rheometer (TA rheometer), the results were shown in **Figure 3.** Apparently, the 1wt% SA solution behaved vary close to a Newtonian fluid, but the 2 wt% SA solution showed a clear shear thinning characteristic at high shear rate. The SA layer was then coated on the surface of dried graphene EAL. The distance between the bottom of the liquid layer and the substrate was guaranteed as 500 μm by applying 10 layers of tape.

2.3 Design of the experiments

TABLE 1. *Design of experiments*

Liquid layer material	Number of EAL layer	Laser pulse energy (μJ)
1% SA solution	No	6 - 30
	1	6 - 30
	2	6 - 30
2% SA solution	No	6 - 30
	1	6 - 30
	2	6 - 30

As summarized in **Table 1**, several experiments were conducted in this study. Printing with and without graphene EAL was used to investigate the effect of graphene EAL on the jet generation process. Additionally, the effect of EAL thickness was investigated by using single layer ~~of~~ graphene EAL and double layers ~~of~~ graphene EAL. In this study, based on the calculation of the volume of graphene solution, 10 μL of graphene disperse solution was considered as a single EAL after it was dried, and 20 μL of graphene solution was considered as two layers of EALs after it was completed dried. To explore the effect of viscosity for SA on the LIFT printing process, 1 wt% and 2 wt% SA solutions were selected. In all experiments, the volume of the SA solution was 20 μL; this actually maintained the layer thickness of SA as 100 μm since the coating area was fixed. During the printing process, the high-speed camera was used to record the jet formation process.

2.4 Post printing graphene EAL testing

After the LIFT printing process, small holes appeared in the laser-interaction area on the EAL, apparently these holes were formed due to the loss of graphene because of the laser-liquid interaction. The EAL substrates with holes were then examined using an optical microscope (Axiovert 200 M).

3. Results and discussions

Straight lines were printed on the receiving substrate using SA solution with different concentrations, and the tests also considered the effects of graphene EAL on the jet formation under different pulse laser input energies. The jet generation

process was recorded by the high-speed camera. The comparison of printing quality was based on the shape of the jets and the length of the jets. The recorded images of the jets at different instants during the LIFT printing process were shown in **Fig. 4** and **Fig. 5**, and a detailed comparison of jet length at various time instants with different laser energies was shown in **Fig. 6**. The microscope images of the holes on the EAL after the interaction were shown in **Fig. 7**.

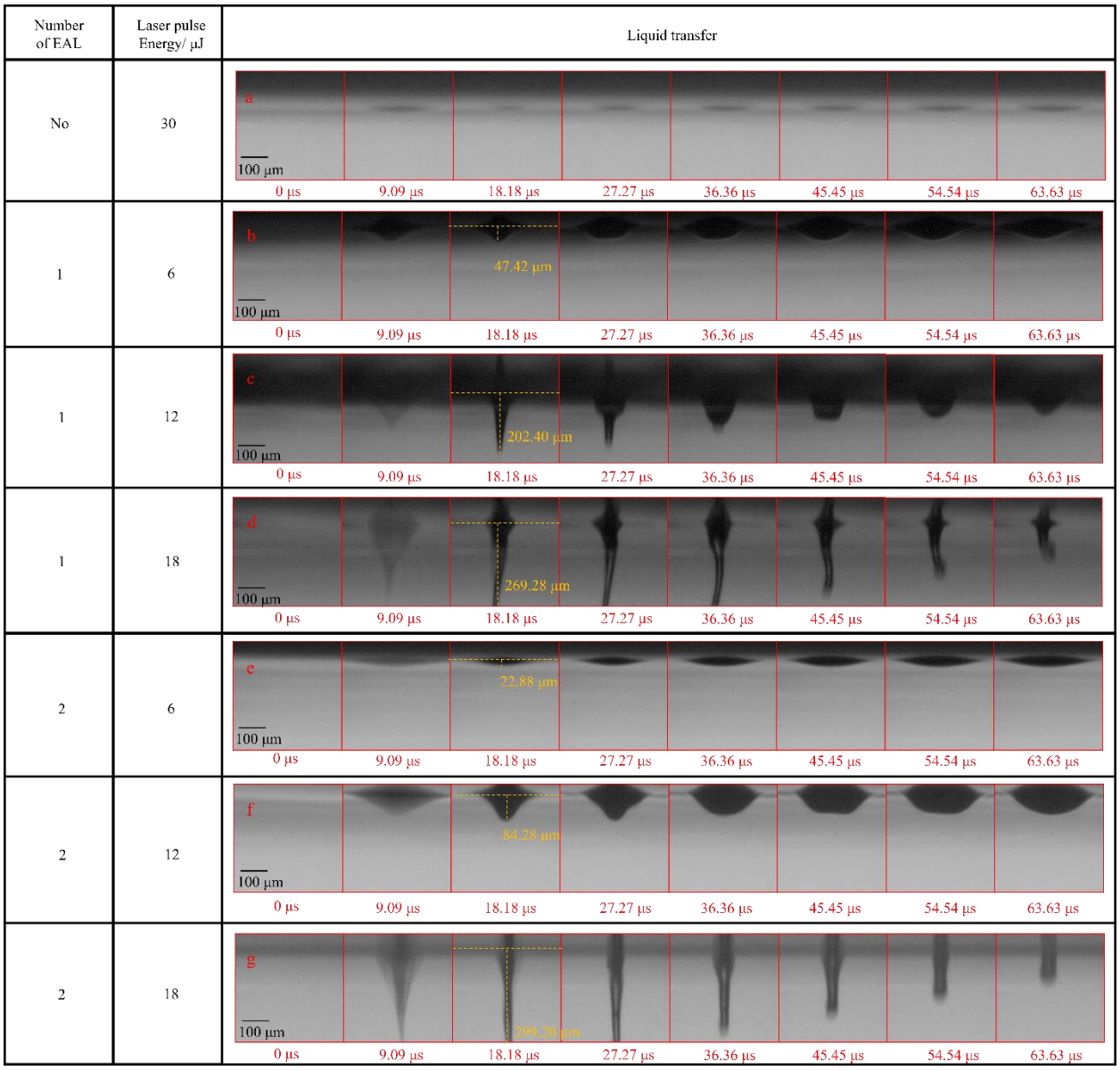

Fig. 4. *The generation of jet during the LIFT process using 1% sodium alginate*

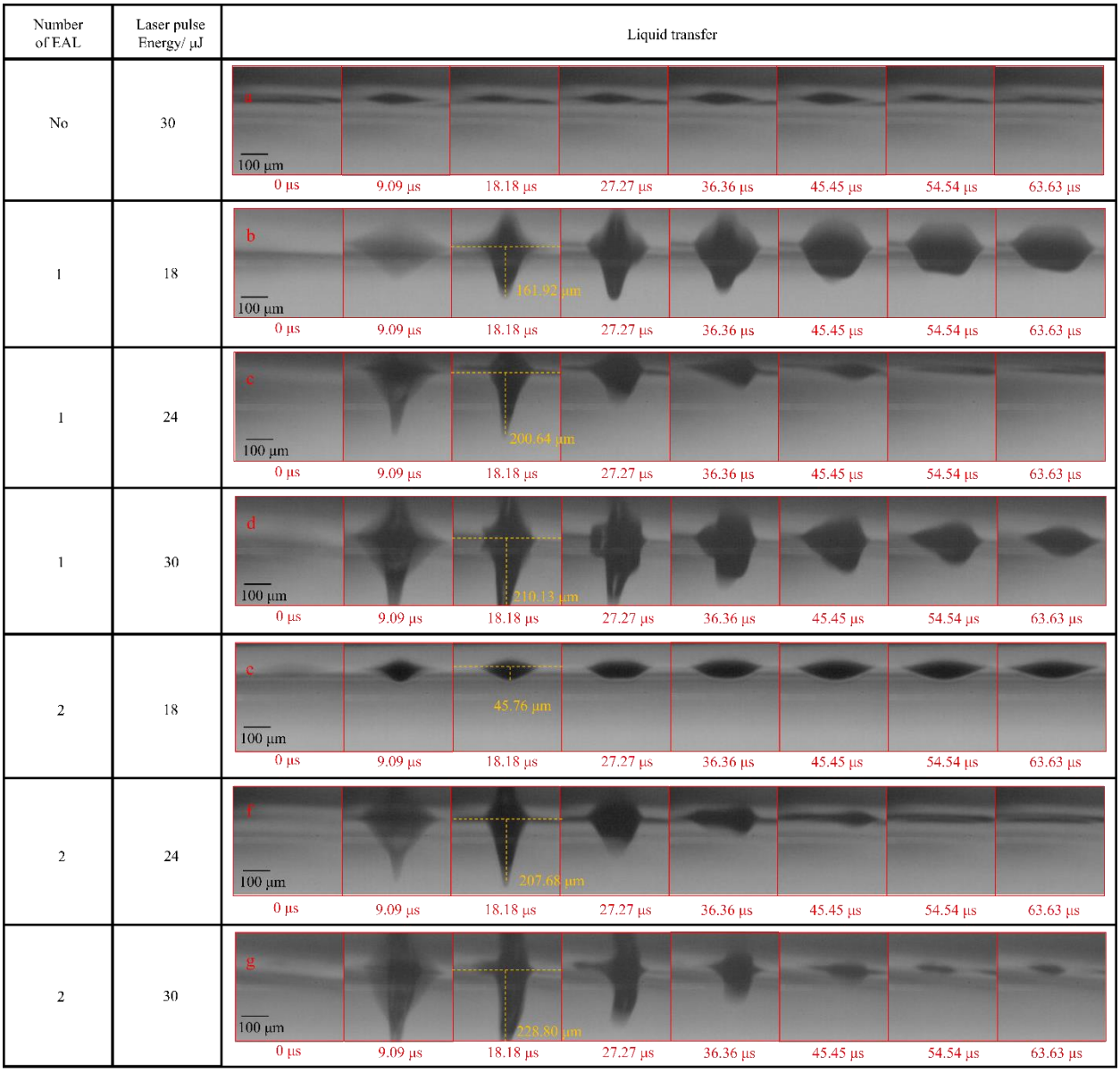

Fig. 5. *The generation of jet during the LIFT process using 2% sodium alginat*

3.1 Effect of graphene EAL on the jet generation in the LIFT bioprinting process

Comparing **Fig. 4 (a)** and **(c)**, it can be found that when using the 1wt% SA solution, even though the laser pulse energy was 30 μJ, there was still no observable jet. When a graphene EAL was applied, there was a stable jet when the laser pulse energy was only 12 μJ. This means that with the application of graphene EAL the laser pulse energy needed to generate a jet was reduced significantly when using the 1wt% SA. Similarly, the same conclusion can be drawn from the comparison between **Fig. 5 (a)** and **(b)**, in which the jet was not generated under 30 μJ laser pulse energy without a graphene EAL, but it was generated under 18 μJ with the application of graphene EAL when using the 2 wt% SA solution. Those results suggest that unlike other EAL materials (e.g. Au, Ag, …), the graphene EAL can help reduce the required laser energy for jet formation, and the range of printing materials can be greatly extended when adopting the graphene solution as the EAL, because the graphene EAL can significantly increase the laser energy absorption. Consequently, other polymers can also be adopted for stable jet formation as long as the laser energy absorption rate can be enhanced. Another potential benefit of using graphene EAL is that the graphene is carbon, as discussed in Section-1 Introduction, there is less concern about the triggered abnormal immune responses when applied in cell printing.

Moreover, the thickness of EAL was directly connected to

the jet regime during the LIFT process. The thickness of graphene EAL was measured by the optical microscope, the average thickness of the single EAL was about 8 μm, and about 15 μm for the double layer EALs.

Comparing **Fig. 4 (b - g)**, the results show that for a single EAL layer, the minimum required laser energy to generate a stable jet is 12 uJ, which is lower than that for double-layer EAL case (18 uJ). Apparently, for those cases without enough laser energy input, only bubbles were observed, no jets can be formed to transfer the SA to the receiving substrate. From **Fig. 6 (a)**, once a stable jet was formed with relatively high laser energy inputs, the jet length tends to be very close between single EAL case and double-layer EAL case. For example, when laser energy was 18 uJ, the maximum jet length is 269.29 μm for single EAL case, and double-layer EAL case has about 299.2 μm maximum jet length. However, the difference among other cases is more significant when a stable jet is not formed. Similar phenomenon can be observed in 2wt% SA solution from **Fig. 6 (b)** (210.17 um for 30uJ / single EAL case and 228.80 um for 30uJ / double0layer EAL case). This may attribute to the heat transfer effect on the EAL, since thicker EAL may absorb more laser energy thank thinner EAL in the same time period, but at the same time, the associated heat loss for thicker EAL case may be greater than the thinner EAL case. Consequently, there may exist a threshold value for input laser energy to form a longer jet to transfer the SA solution. If the input laser energy exceeds the threshold, the net absorbed energy for a thicker EAL may be larger than that of a thinner EAL, thus leading to a longer jet. These findings may help modify the design of EAL in the future.

3.2 Effect of the viscosity of SA bioink on the jet generation in LIFT bioprinting

The dynamic viscosity of the 2 wt% SA solution used in this study was around 2.321 Pa·S, and the dynamic viscosity of 1 wt% SA solution was about 0.473 Pa·S. By comparing **Fig. 4 (c)** and **Fig. 5 (b)**, it can be found that when a single EAL was attached, the laser pulse energy required to generate a jet was higher than that in 1 wt% SA solution (18 μJ and 12 μJ, respectively). This conclusion also applies to double EAL cases (**Fig. 4 (g)** and **Fig. 5 (f)**). By comparing **Fig. 6 (a)** and **(b),** it can also be found that the laser energy input required to achieve a jet of same length for 2wt% SA is much higher than the required energy for 1wt% SA. It indicates that with higher viscosity, more laser energy is required to transfer the liquid to the receiving substrate, which may challenge the printability and the required laser input energy.

In the LIFT process, the maximum length of the jet will also influence the printing quality, since if the tip of the jet cannot reach the receiving substrate, no material will be transferred. It was observed in this study that for both SA solutions (1 wt% and 2 wt%) after the jet was generated, there was a maximum length of the jet. After reaching the maximum length, the jet bounced back to the top substrate. Nevertheless, this phenomenon cannot be observed in low viscosity fluid, such as water. Therefore, we can conclude that it is easier to maintain a stable jet for a high viscosity fluid when compared to a low viscosity fluid [11].

We can also observe that the maximum length (210.13 μm for single EAL and 228.80 μm for double EAL) for 2 wt% SA EAL was shorter than that (269.28 μm for single EAL and 299.20 μm for double EAL) of 1 wt% SA EAL, as shown in **Fig. 4 (d)** & **Fig. 5 (d),** and **Fig. 4 (g)** & **Fig. 5 (g)**. Hence, the rheological properties of the solution controlled the jet behavior during the LIFT process. This may occur because of the laser energy irradiated on the high viscosity fluid, and the viscous dissipation was less than that of low viscosity fluid, which may lead to a lower jet velocity. This is also a reason why a shorter jet length, and a more stable jet regime can be observed in high viscosity fluid during the LIFT process.

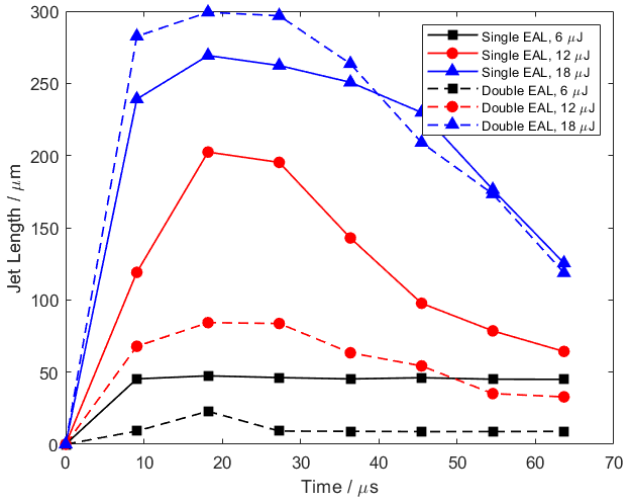

(a)

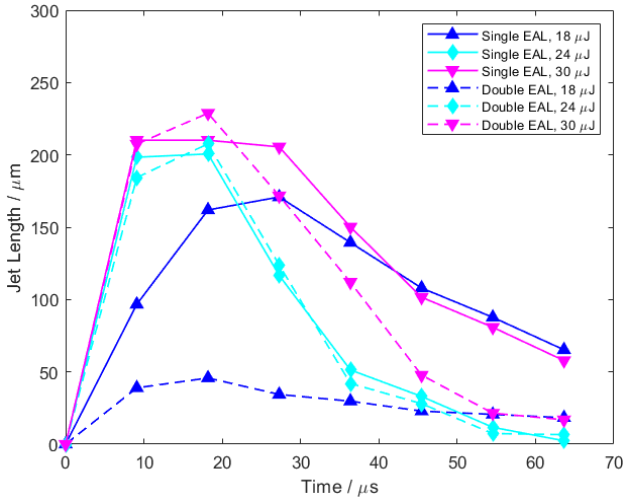

(b)

Fig. 6. *The length of jet during the LIFT process with different energy using (a) 1% sodium alginate solution; (b) 2% sodium alginate solution*

3.3 Analysis and discussion about the holes on the EAL

As shown in **Fig. 7**, microscope images of EAL holes on the substrate showed that there were signs of strong mechanical impact at the edges of these EAL holes, and the impacts were more significant for those holes with a thicker EAL. Therefore, during the LIFT printing process, the effect of EAL mechanical impact may be as important as the heat transfer effect. In particular, the shape of holes from 8 μm EAL showed typical circular shapes, while the holes from 15 μm EAL appeared like a jagged polygon. This phenomenon can be explained by a fact the energy absorbed from the laser is higher for a thicker EAL, which will lead to a severer mechanical impact. Since the impact is more severe in double EAL cases, there may be more fragments of graphene ejecting into the printed droplet, though it is not poisonous to cells when applied in cell printing, it may still influence the cell viability due to the high impact-induced acceleration. Another concern is that the cell structure may be changed since cells may adhere to the fragments. These concerns should be clarified in a future study when applying bioink with cells.

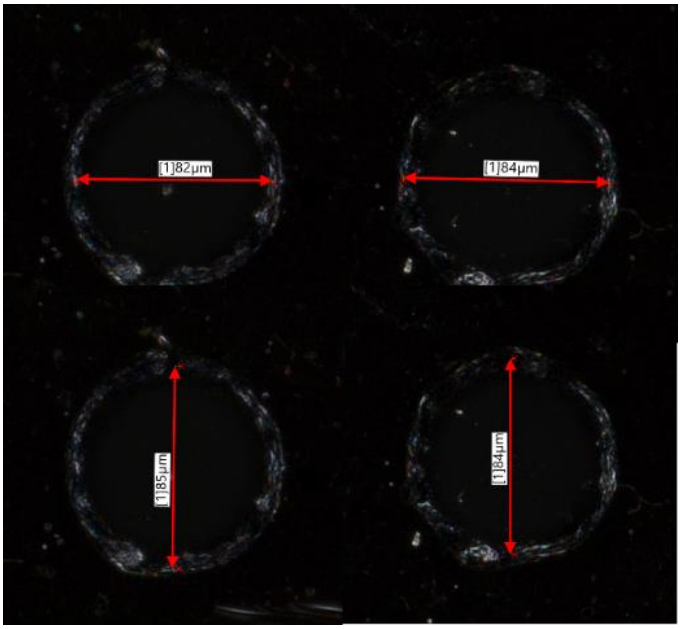

(a) Single EAL

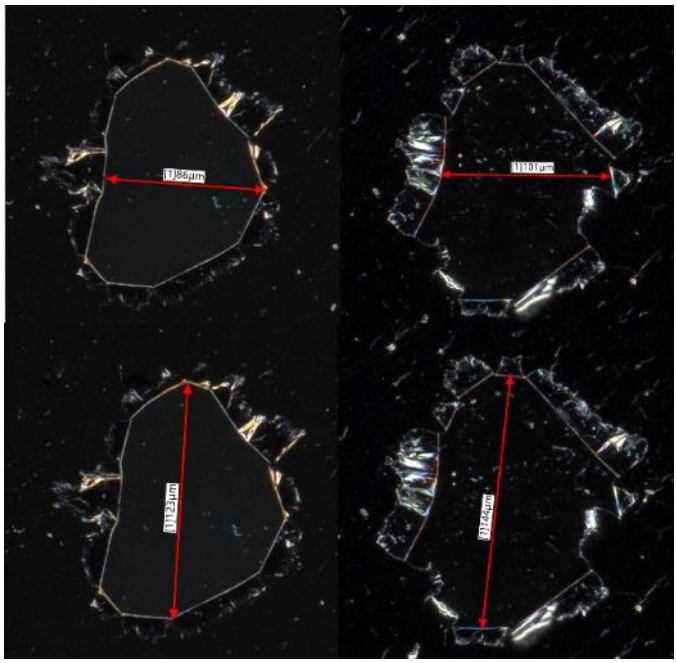

(b) Double EAL

Fig. 7. *Optical Microscope images of holes in the EAL after LIFT printing (The observation surface is the laser output direction)*

4. CONCLUSION

Since the printing quality of LIFT bioprinting is highly dependent on the stability of the jet, it is essential to figure out the factors that influence the jet generation process. In this study, we find that the graphene EAL can assist to generate the jet to transfer bioink with a low laser energy absorption rate (such as transparent SA solutions) which may attribute to the facilitation of heat transfer and the mechanical impact of EAL. The thickness of graphene EAL also influences the jet formation. The viscosity of the SA solution also plays a significant role in the generation of a stable jet for material transfer. For the cases with the same laser energy input, the jet generated using higher viscosity bioink had a smaller initial velocity; this eventually led to a shorter jet length. The findings in this study will help optimize the setup of EAL and the preparation of bioink, and the results found in this study may help the bioprinting research community to achieve higher cell viability in bioprinting.

ACKNOWLEDGEMENTS

The authors are grateful for the financial support to this work from the start-up fund at Mississippi State University. Special thanks are due to Dr. Kundu in the School of Chemical Engineering at Mississippi State University for providing the viscometer to measure the viscosity of SA solutions. We also

would like to thank Carter Berry for proofreading the manuscript.

REFERENCES

[1] Mandrycky, C., Wang, Z., Kim, K., & Kim, D. H. (2016). 3D bioprinting for engineering complex tissues. Biotechnology advances, 34(4), 422-434.

[2] Moroni, L., Boland, T., Burdick, J. A., De Maria, C., Derby, B., Forgacs, G., ... & Vozzi, G. (2018). Biofabrication: a guide to technology and terminology. Trends in biotechnology, 36(4), 384-402.

[3] Dou, C., Perez, V., Qu, J., Tsin, A., Xu, B., & Li, J. (2021). A State-of-the-Art Review of Laser-Assisted Bioprinting and its Future Research Trends. ChemBioEng Reviews, 8(5), 517-534.

[4] Antoshin, A. A., Churbanov, S. N., Minaev, N. V., Zhang, D., Zhang, Y., Shpichka, A. I., & Timashev, P. S. (2019). LIFT-bioprinting, is it worth it?. Bioprinting, 15, e00052.

[5] Morales, M., Munoz-Martin, D., Marquez, A., Lauzurica, S., & Molpeceres, C. (2018). Laser-induced forward transfer techniques and applications. Advances in Laser Materials Processing, 339-379.

[6] Murphy, S. V., & Atala, A. (2014). 3D bioprinting of tissues and organs. Nature biotechnology, 32(8), 773-785.

[7] Guillotin, B., Souquet, A., Catros, S., Duocastella, M., Pippenger, B., Bellance, S., ... & Guillemot, F. (2010). Laser assisted bioprinting of engineered tissue with high cell density and microscale organization. Biomaterials, 31(28), 7250-7256.

[8] Zhang, Z., Xiong, R., Mei, R., Huang, Y., & Chrisey, D. B. (2015). Time-resolved imaging study of jetting dynamics during laser printing of viscoelastic alginate solutions. Langmuir, 31(23), 6447-6456.

[9] Qu, J., Dou, C., Li, J., Rao, Z., & Xu, B. (2020, July). Numerical and Experimental Study of Bioink Transfer Process in Laser Induced Forward Transfer (LIFT) 3D Bioprinting. In Heat Transfer Summer Conference (Vol. 83709, p. V001T08A002). American Society of Mechanical Engineers.

[10] Qu, J., Dou, C., Xu, B., Li, J., Rao, Z., & Tsin, A. (2021). Printing quality improvement for laser-induced forward transfer bioprinting: Numerical modeling and experimental validation. Physics of Fluids, 33(7), 071906.

[11] Smausz, T., Hopp, B., Kecskeméti, G., & Bor, Z. (2006). Study on metal microparticle content of the material transferred with absorbing film assisted laser induced forward transfer when using silver absorbing layer. Applied surface science, 252(13), 4738-4742.

[12] Doraiswamy, A., Narayan, R. J., Lippert, T., Urech, L., Wokaun, A., Nagel, M., ... & Chrisey, D. B. (2006). Excimer laser forward transfer of mammalian cells using a novel triazene absorbing layer. Applied Surface Science, 252(13), 4743-4747.

[13] Catros, S., Fricain, J. C., Guillotin, B., Pippenger, B., Bareille, R., Remy, M., ... & Guillemot, F. (2011). Laser-assisted bioprinting for creating on-demand patterns of human osteoprogenitor cells and nano-hydroxyapatite. Biofabrication, 3(2), 025001.

[14] Koch, L., Deiwick, A., Franke, A., Schwanke, K., Haverich, A., Zweigerdt, R., & Chichkov, B. (2018). Laser bioprinting of human induced pluripotent stem cells—the effect of printing and biomaterials on cell survival, pluripotency, and differentiation. Biofabrication, 10(3), 035005.

[15] Koch, L., Deiwick, A., & Chichkov, B. (2014). Laser-based 3D cell printing for tissue engineering. BioNanoMaterials, 15(3-4), 71-78.

[16] Haider, A. J., Haider, M. J., Majed, M. D., Mohammed, A. H., & Mansour, H. L. (2017). Effect of laser fluence on a microarray droplets micro-organisms cell by LIFT technique. Energy Procedia, 119, 256-263.

[17] Lin, Y., Huang, Y., & Chrisey, D. B. (2011). Metallic foil-assisted laser cell printing. Journal of biomechanical engineering, 133(2).

[18] Smausz, T., Hopp, B., Kecskeméti, G., & Bor, Z. (2006). Study on metal microparticle content of the material transferred with absorbing film assisted laser induced forward transfer when using silver absorbing layer. Applied surface science, 252(13), 4738-4742.

[19] Zennifer, A., Subramanian, A., & Sethuraman, S. (2022). Design considerations of bioinks for laser bioprinting technique towards tissue regenerative applications. Bioprinting, e00205.

[20] Bijukumar, D. R., Segu, A., Souza, J. C., Li, X., Barba, M., Mercuri, L. G., ... & Mathew, M. T. (2018). Systemic and local toxicity of metal debris released from hip prostheses: A review of experimental approaches. Nanomedicine: Nanotechnology, Biology and Medicine, 14(3), 951-963.

[21] Peña-Bahamonde, J., Nguyen, H. N., Fanourakis, S. K., & Rodrigues, D. F. (2018). Recent advances in graphene-based biosensor technology with applications in life sciences. Journal of nanobiotechnology, 16(1), 1-17.

[22] Li, Q., Lu, J., Gupta, P., & Qiu, M. (2019). Engineering optical absorption in graphene and other 2D materials: advances and applications. Advanced Optical Materials, 7(20), 1900595.

[23] Yan, J., Huang, Y., Xu, C., & Chrisey, D. B. (2012). Effects of fluid properties and laser fluence on jet formation during laser direct writing of glycerol solution. Journal of Applied Physics, 112(8), 083105.

[24] Zhang, Z., Xiong, R., Corr, D. T., & Huang, Y. (2016). Study of impingement types and printing quality during laser printing of viscoelastic alginate solutions. Langmuir, 32(12), 3004-3014.

[25] Mazumdar, J. (2015). Biofluid mechanics. World Scientific.